

Thermal Scattering Law for Zirconium Hydride

I. Švajger¹, N. C. Fleming², G. Noguere³, A. I. Hawari², L. Snoj¹, A. Trkov¹

¹ "Jozef Stefan" Institute
Jamova cesta 39
1000, Ljubljana, Slovenia

ingrid.svajger@ijs.si, luka.snoj@ijs.si, andrej.trkov@ijs.si

² North Carolina State University
3140 Burlington Engineering Labs, 2500 Stinson Drive
NC 27695-7909, Raleigh, USA

ncsorrel@ncsu.edu, ayman.hawari@ncsu.edu

³ CEA, DeS, DER, Experimental physics, Safety experiment and Instrumentation
Section

13108 Saint Paul-lez-Durance
Cadarache, France

gilles.noguere@cea.fr

ABSTRACT

This study aims to evaluate the thermal neutron scattering properties of zirconium hydride (ZrH_x), focusing on the ϵ -phase ($x = 2$) and δ -phase ($x = 1.5$). The methodology included density functional theory calculations using the VASP code to derive force constants, followed by Phonopy code and NJOY for lattice dynamics and thermal scattering properties. Key results of this research include precise atomic structures, mechanical properties, and thermal scattering cross sections. Thermal scattering cross section for ϵ - and δ -phases of ZrH_x , along with comparisons to ENDF/B-VIII.0 shows that the total and elastic spectra have similar shapes, but differences become more pronounced in the inelastic part, both in shape and size.

1 INTRODUCTION

In recent years, with advances in computing power, state-of-the-art atomistic simulations based on first principles have become available for use in chemistry and physics. In these simulations, the motion of the crystal lattice or molecules is simulated using algorithms from the field of computational physics, such as density functional theory and its derivatives. The goal is to generate thermal neutron scattering cross sections and the corresponding covariance matrices. We are mainly interested in the material zirconium hydride ZrH_x , which is used in the numerous research reactors like TRIGA. TRIGA reactors have a unique fuel composition: a homogeneous mixture of 20% enriched uranium and zirconium hydride (ZrH ratio close to 1.6). This is the main reason for the prompt negative temperature reactivity coefficient. Since the hydrogen in the zirconium hydride acts as a moderator, most of the moderation occurs in the fuel element itself and only a small part in the water surrounding the fuel elements. Therefore, any change in power and fuel temperature directly affects the moderator in the fuel element. In this case, the fuel and moderator directly affect the reactivity of the core. Since hydrogen bound in a crystal lattice is an essential feature of hydride fuelled

reactors, accurate modelling of reactor behaviour is directly limited by the quality of thermal neutron scattering nuclear data.

ZrH_x can exist in several phases with different stoichiometries, of which the δ -phase (dominant at room temperature for $1.56 < x < 1.64$) and the ϵ -phase (dominant at room temperature for $x > 1.74$) are the most important. The purpose of this paper is to evaluate our computational method and compare our results with the current thermal neutron scattering law data from the ENDF/B- VIII.1 library. The current ENDF/B- VIII.1 ZrH_x nuclear data evaluations do not distinguish between phases. The thermal neutron scattering law data for ZrH_x from the ENDF/B-VIII.0 library were generated using historical phonon spectra derived from a central force model and assume incoherent elastic scattering for both bound hydrogen and zirconium, neglecting the effects of crystal structures that are important for the scattering of zirconium bound in ZrH_x. Thermal neutron scattering laws for $x = 1.5$ and $x = 2$ were established and compared with the ENDF/B- VIII.1 library.

2 THERMAL NEUTRON SCATTERING

In the low neutron energy range, typically below 5 eV, neutron scattering is affected by the atomic bonding of the scattering molecule in the moderator. Compared to a free nucleus, this changes the reaction cross section and thus the energy and angular distribution of the secondary neutrons. In neutron scattering, a distinction is made between elastic and inelastic scattering. While the former is important, the latter is directly related to reactor applications, since the neutrons must be slowed down to increase the fission probability of the fissile isotopes. Both elastic and inelastic scattering can be coherent or incoherent. In coherent scattering, the interference phenomena between waves reflected from nearby nuclei affect the scattering target. [2]

The importance of the elements varies depending on the state of the scatterer (liquid, solid) and the properties of the material. In hydrogen-rich materials such as zirconium hydride, yttrium hydride, polyethylene, or water, incoherent elastic scattering plays a crucial role due to the strong cross-sectional interaction of hydrogen atoms. Crystalline materials such as graphite, beryllium, and uranium dioxide rely on coherent elastic scattering because it affects the angular distribution of the scattered neutrons. Meanwhile, inelastic scattering is important for all types of materials. [2]

For many materials, only inelastic scattering is considered in the calculation of thermal neutron cross sections, which are then used in nuclear data processing codes. The inelastic double differential effective cross section can be calculated with the well-known formula:

$$\frac{d^2\sigma}{d\Omega dE'} = \frac{1}{4\pi k_B T} \sqrt{\frac{E'}{E}} e^{-\frac{\beta}{2}} (\sigma_{coh} S(\alpha, \beta) + \sigma_{inc} S_s(\alpha, \beta)), \quad (1)$$

where E is the neutron flux energy, Ω is the direction, E' is the secondary energy, Ω' is the direction, σ_{coh} and σ_{inc} are the coherent and incoherent scattering cross sections, k_B is the Boltzmann constant, T is the temperature of the material and $S(\alpha, \beta)$ is the thermal scattering function. The thermal scattering function $S(\alpha, \beta)$ is given by the equation:

$$S(\alpha, \beta) = S_s(\alpha, \beta) + S_d(\alpha, \beta) \quad (2)$$

In the above equation $S_s(\alpha, \beta)$ represents the self-scattering function that accounts for non-interference or incoherent effects, while $S_d(\alpha, \beta)$ represents the distinct-scattering function that accounts for interference or coherent effects. The scattering law is a function of the dimensionless momentum transfer α and energy transfer β given with these two equations:

$$\alpha = \frac{E' + E - 2\sqrt{E'E}\mu}{Ak_B T}, \quad (3)$$

$$\beta = \frac{E' - E}{k_B T} = \frac{\hbar\omega}{k_B T}. \quad (4)$$

In these equations μ represents the cosine of the scattering angle in the laboratory system and A is the ratio between the mass of the scattering target M and the neutron mass m . The energy transfer $E'-E$ is sometimes denoted as the product between the reduced Planck's constant \hbar and the excitation frequency ω . [1]

The scattering law is a fundamental quantity of the scattering system. The dynamics of the scattering law can be approximated in two ways: via the Van Hove space-time self-correlation function or, better, via its Fourier transform in time - the intermediate scattering function. However, since these cannot be calculated explicitly for systems of practical interest, the phonon expansion is used instead. The main point of the expansion is that the thermal scattering law is written as a sum of partial thermal scattering laws S_p , where $p = 0, 1, 2, \dots$ stands for the scattering interaction in which the neutron interacts with p phonons. The term $p=0$ is the one where there is no energy exchange, so S_0 corresponds to elastic scattering, S_1 to inelastic scattering where one phonon is exchanged, etc. [2]

With the advent of advanced computer simulations, it became possible to simulate an ensemble of atoms or molecules and obtain the interatomic force constants from first principles. The double differential thermal neutron scattering cross section consists of two parts: the interaction between neutrons and nuclei, represented by the bound atom cross section and a factor, that considers the dynamics of the scattering system, represented by the dynamic structure factor. In most cases, the scattering law for crystalline materials is calculated using the phonon expansion in incoherent approximation, where the distinct-scattering term of the scattering law is set to zero. The incoherent approximation (mostly) holds so well because, in multiphonon scattering, for almost any energy and/or momentum transfer, there are a large number of combinations of multiple phonons that satisfy the energy and crystal momentum conservation relations. This approximation is sufficient for many materials of interest, but this assumption can lead to inaccuracies in the calculated cross section for materials such as graphite and beryllium. Fortunately, the missing coherent inelastic contribution can be introduced separately into the expression by various methods. In addition, an extension of the ENDF format to include a coherent and an incoherent contribution is currently being prepared. In crystalline solids, phonons are the main excitation mode responsible for the energy exchange between the neutron and the material, and if other contributions are neglected, the calculation of the differential and total cross sections can be reduced to the calculation of the phonon density of states, from which all other quantities can be calculated. [2]

3 COMPUTATIONAL METHOD

The density of states can be extracted from a simulated motion of an atomic or molecular system. Based on the extracted density of states, thermal nuclear data (TND) can be calculated. In density functional theory (DFT), the total electronic force is the sum of the Coulomb repulsion between nuclei and the quantum mechanical electron potential, which itself consists of electron-electron interactions and electron-atom interactions. A basic assumption of DFT is that the total energy of the electronic system can be expressed as a function of the electronic density and that the ground state of the system can be obtained by minimising the function. In principle, the success of DFT is due to the fact that there is a bijective transformation between the wave functions of the constituent electrons and the full electron density of the molecule: The many-electron problem is reduced to a one-electron problem. To accurately simulate the behaviour of an atomic or molecular system, the interatomic (intermolecular) potential must be known so that the forces on the individual atoms (molecules) can be calculated.

The system is modelled and relaxed to its ground state using the density functional theory capable computer code VASP [3]. The positions of the atoms are then perturbed and the interatomic force constants are calculated. Once the force constants are obtained, they are transferred to the Phonopy code [4], which performs lattice dynamics calculations to find solutions to the dynamical matrix problem. The solutions form the dispersion relations of the system, from which the atomic vibrational density of states is computed using a geometrical sampling procedure. Once the density of states is known, the scattering law and all associated quantities can be calculated using the LEAPR module of the NJOY data processing system [5]. The scattering law data are the basis for the analysis of thermal reactor systems, which are often modelled using Monte Carlo transport codes to obtain the desired physical reactor parameters.

In this approach the dynamical matrix calculation is only strictly valid at 0 K, which means the phonon density of states (DOS) obtained does not capture temperature dependent effects such as phonon softening and anharmonicity of the lattice. Also, materials which are non-periodic (not a crystal) cannot be treated.

Total energy calculations are self-consistently carried out using density functional theory (DFT) as implemented in Vienna ab initio simulation package (VASP) [6], which is based on pseudopotentials and plane wave basis functions. All electron projected augmented wave (PAW) method of Blöchl [7] is applied in VASP with the frozen core approximation. The generalized gradient approximation (GGA) introduced by Perdew, Burke, and Ernzerhof (PBE) [8] is employed to evaluate the electron exchange and correlation potential. Zirconium $4s^2 4p^6 4d^2 5s^2$ and hydrogen $1s^1$ electrons are treated as valence electrons. The integration over the Brillouin Zone is performed with a grid of special k point-mesh determined according to the Monkhorst–Pack scheme [9].

3.1 Convergence test

Convergence test is used to test model to be fully converged. Appropriate convergence of planewave energy cutoff and k-point mesh is determined by tracking three specific outputs of the VASP calculation: unit cell volume V ($\frac{\Delta V}{V} < 0.1\%$), energy E ($\Delta E < 5 \frac{meV}{atom}$) and pressure p ($\frac{\Delta P}{P} < 1\%$). According to the convergence test, a k-point mesh of $13 \times 13 \times 13$ and a cutoff energy of 675 eV is chosen for the ϵ -phase, while a k-point mesh of $10 \times 10 \times 10$ and a cutoff energy of 675 eV is chosen for the δ -phase. The self-consistent convergence of the total energy calculation is set to 10^{-8} eV.

3.2 Atomic structure

At ambient conditions, the stable zirconium dihydride (ϵ -phase) crystallizes in a tetragonal crystal structure with space group I4/mmm. In its unit cell there are two Zr atoms with position (0, 0, 0) and four H atoms with position (0, $\frac{1}{2}$, $\frac{1}{4}$) (see Figure 1). Each Zr atom is surrounded by eight H atoms to form a tetragonal cell, and each H atom combines with four Zr atoms to form a tetrahedron. The current optimized equilibrium lattice parameters (a and c) are 3.540 Å and 4.408 Å, respectively.

On the other hand ϵ -phase is a face-centered cubic phase with Fm3-m space group. In its unit cell, there are four Zr atoms with position (0, 0, 0) and six H atoms randomly occupying the eight available tetragonal ($\frac{1}{4}$, $\frac{1}{4}$, $\frac{1}{4}$) sites (see Figure 1). The current optimized equilibrium lattice parameter ($a=b=c$) is 4.776 Å. Equilibrium lattice parameters for ϵ and δ phase are in agreement with the experimental values (see Table 1).

Table 1: Calculated lattice constants for ϵ and δ phase. For comparison available experimental values.

property	a [Å]	c [Å]
ϵ -phase	3.540	4.408
ϵ -phase – experiment [10]	3.522	4.451
δ -phase	4.776	
δ -phase – experiment [11]	4.771	

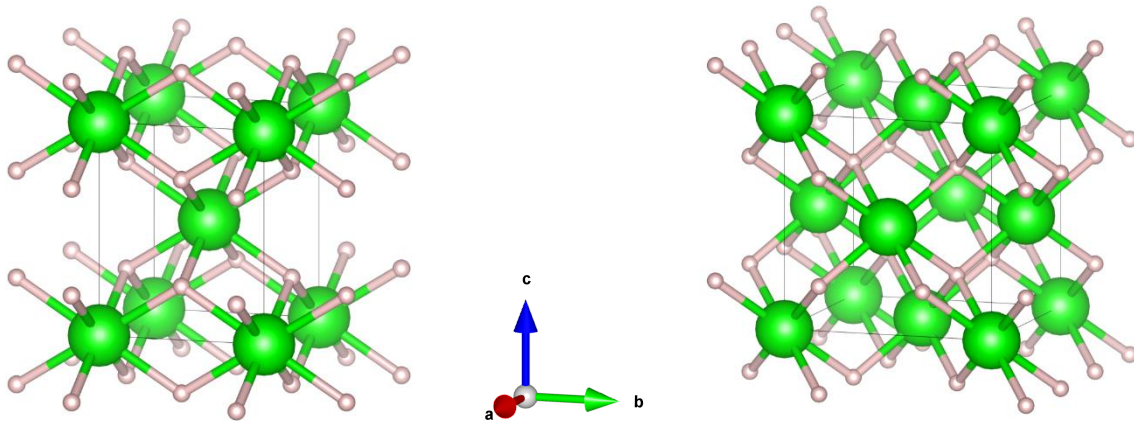


Figure 1: Unit cells for ϵ -phase left and δ phase right. Green spheres present Zr atoms and white spheres presents H atoms.

4 RESULTS

In this chapter, the results of mechanical properties, elastic constants, bulk modulus, shear modulus, and Young modulus, and thermal scattering cross sections for the ϵ - and δ -phase of ZrH are presented. The mechanical properties are compared with calculations from other literatures and with experimental data. The thermal scattering cross sections for both phases are compared with existing ENDF/B- VIII.1 thermal scattering cross section and with calculations from the literature.

4.1 Mechanical properties

This chapter focuses on exploring the mechanical properties to validate our models. This is important because atomic structure and potentials play a role in affecting these mechanical properties. Among these properties, the elastic constants play an important role in quantifying the response of a crystal to external stresses or pressure, thus providing information about its mechanical properties. The determination of six independent elastic constants, namely C_{11} , C_{12} , C_{13} , C_{33} , C_{44} , and C_{66} , is crucial. Once these elastic constants are known for a material, it is possible to calculate the bulk modulus (K), shear modulus (G) and Young's modulus (E) for various hydrides using the established relationships between K , G and E :

$$K = \frac{1}{9}(C_{11} + C_{22} + C_{33} + 2(C_{12} + C_{13} + C_{23})), \quad (5)$$

$$G = \frac{1}{15}(C_{11} + C_{22} + C_{33} + 3(C_{44} + C_{55} + C_{66}) - C_{12} - C_{13} - C_{23}), \quad (6)$$

$$E = \frac{9KG}{3K + G}. \quad (7)$$

Comparing bulk modulus, shear modulus, and Young's modulus is a widely used approach, as opposed to comparing elastic constants. The corresponding values for these parameters are listed in Table 2.

Table 2

Table 2: Calculated bulk modulus, shear modulus and Young modulus.

	K [GPa]	G [GPa]	E [GPa]
ϵ -phase	134.2	35.6	98.1
ϵ -phase from [12]	130	29	80
δ -phase	124	10	30
δ -phase experiment [11]	128	24	69
δ -phase experiment [13]	125	53	138

4.2 Thermal scattering cross section

The thermal scattering cross section is a crucial parameter for understanding and influencing the behaviour of neutrons at low energies. In the following, the thermal scattering cross sections for hydrogen (H) in ZrH are presented for both the ϵ - and δ -phases and compared with the ENDF/B-VIII.0 library [14]. The latest nuclear data evaluations for ZrH_x in the ENDF/B-VIII.0 library do not distinguish between different phases. The thermal neutron scattering law data for ZrH_x in this library were calculated based on historical phonon spectra derived from a central force model. These calculations assume incoherent elastic scattering for both bound hydrogen and zirconium and overlook the influences of crystal structures, which play an important role in the scattering behaviour of zirconium within ZrH_x.

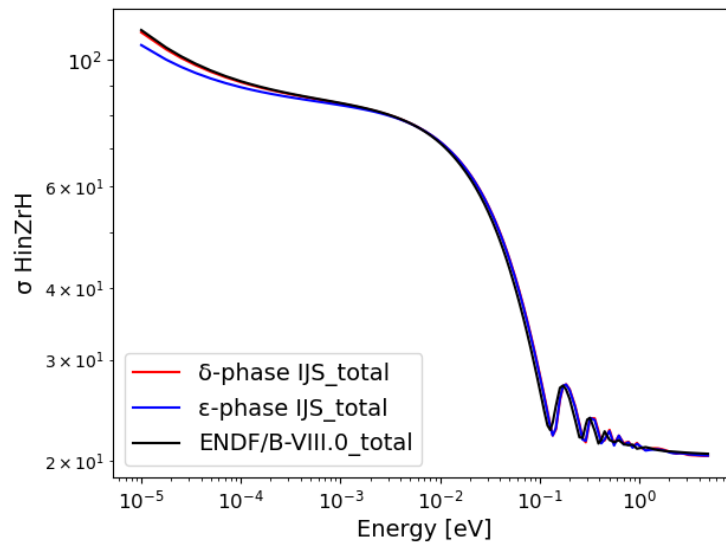


Figure 2: Total thermal scattering cross section.

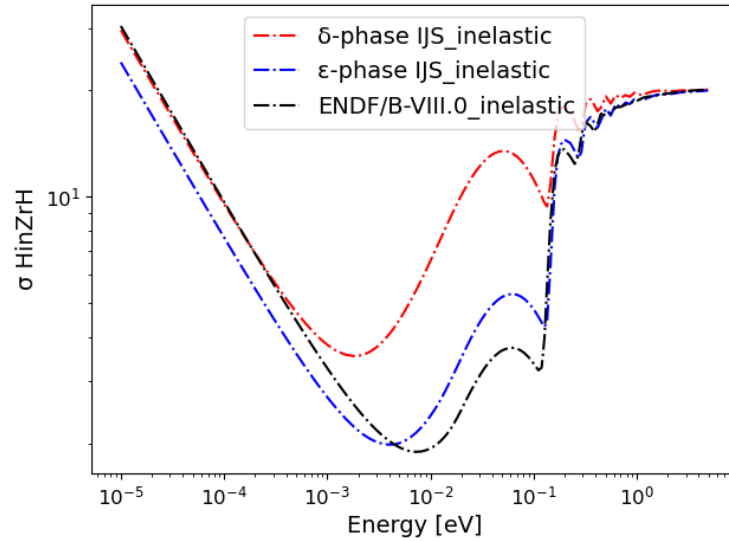


Figure 3: Inelastic thermal scattering cross section.

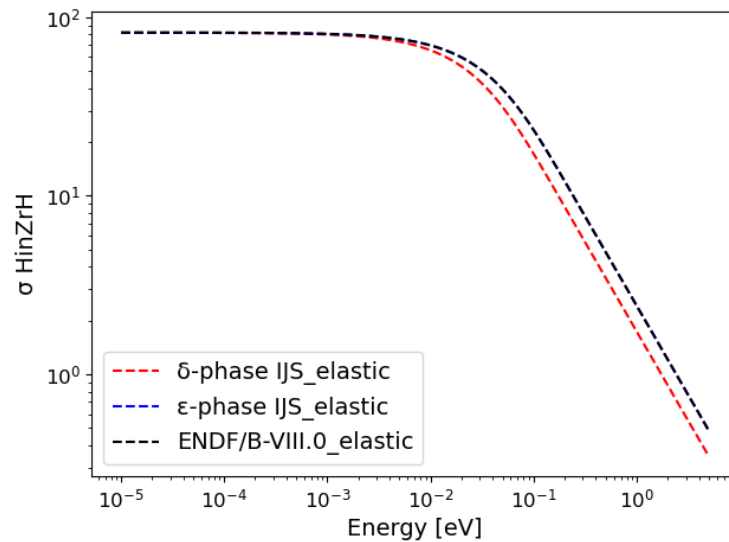


Figure 4: Elastic thermal scattering cross section.

In the plots in Figure 2, Figure 3 and Figure 4, the thermal scattering cross sections for the ϵ -phase are shown in red, the δ -phase in blue, and ENDF/B- VIII.1 in black. For each thermal scattering cross section, the total cross section is shown at Figure 2, the inelastic part at Figure 3, and the elastic part at Figure 4. It can be seen that the total and elastic parts of the spectrum have comparable shapes and are very similar. However, in the inelastic part of the spectrum, the differences become more pronounced. Although the overall shape remains similar, the differences in size are more pronounced.

CONCLUSION

In summary, this study aims to evaluate the thermal neutron scattering properties of zirconium hydride (ZrH_x), focusing on the ϵ -phase and δ -phase, where the δ -phase corresponds to $x = 1.5$ and the ϵ -phase corresponds to $x = 2$. Understanding the scattering properties of these phases is critical as they are found in different reactor configurations. Advanced computational methods based on density functional theory (DFT) and phonon dynamics were used to comprehensively analyse the scattering behaviour of hydrogen-bonded zirconium hydride. The methodology included DFT calculations using the VASP code to derive

force constants, followed by Phonopy code and NJOY for lattice dynamics and thermal scattering properties.

Key results of this research include precise atomic structures, mechanical properties, and thermal scattering cross sections, which are important for nuclear reactor modelling and safety assessments. Detailed descriptions of the ϵ -phase and δ -phase of ZrH_x , including their respective unit cells and equilibrium lattice parameters, were presented, showing good agreement with experimental values. In addition, the study addressed the mechanical properties of ZrH_x , including elastic constants, bulk modulus, shear modulus, and Young's modulus.

Plots of the thermal scattering cross sections for both the ϵ - and δ -phases of ZrH_x , as well as comparisons with ENDF/B-VIII.0, provide insight into neutron behaviour at low energies and serve as an important basis for reactor simulations. The total and elastic spectra have similar shapes, but differences become more pronounced in the inelastic part, both in shape and size. This research contributes significantly to our understanding of neutron behaviour in complex materials, enhances nuclear data repositories, and ultimately improves nuclear reactor safety and performance assessments.

REFERENCES

1. A. I. Hawari, I. I. Al-Qasir, V. H. Gillette, B. W. Wehring, T. Zhou, Ab Initio Generation of Thermal Neutron Scattering Cross Sections, Physor 2004, Chicago.
2. J. C. Holmes, Monte Carlo Calculation of Thermal Neutron Inelastic Scattering Cross Section Uncertainties by Sampling Perturbed Phonon Spectra, Raleigh, North Carolina, (2014).
3. G. Kresse, J. Furthmüller, Phys. Rev. B 54 (1996) 11169.
4. Togo, A., Scr. Mater., 108, 1-5, 2015.
5. Macfarlane, R., The NJOY Nuclear Data Processing System, Version 2016, LA-UR-17-20093.
6. G. Kresse, J. Furthmüller, Phys. Rev. B 54 (1996) 11169.
7. P.E. Blöchl, Phys. Rev. B 50 (1994) 17953.
8. J.P. Perdew, K. Burke, M. Ernzerhof, Phys. Rev. Lett. 77 (1996) 3865.
9. H.J. Monkhorst, J.D. Pack, Phys. Rev. B 13 (1972) 5188.
10. H. E. Flotow, D. W. Osborne, Heat Capacities and Thermodynamic Functions of ZrH_2 and ZrD_2 from 5 to 350°K and the Hydrogen Vibration Frequency in ZrH_2 , The journal of chemical physics, October (1960).
11. Blomqvist, J., Olofsson, J., Alvarez, A.-M., & Bjerkén, C. (2013). Structure and Thermodynamical Properties of Zirconium hydrides from First-Principle. *Journal of Nuclear Materials*, 441(1-3), 473-480.
12. P. Zhang, B. T. Wang, C. H. He, P. Zhang, First-principles study of ground state properties of ZrH_2 , Computational Material Science 50 (2011).
13. P.A.T. Olsson, A.R. Massih, J. Blomqvist, A.-M. Alvarez Holston, C. Bjerkén, Ab initio thermodynamics of zirconium hydrides and deuterides, Computational Materials Science, Volume 86, 2014, Pages 211-222.
14. National Nuclear Data Center, (2022), ENDF/B-VIII.0 Evaluated Nuclear Data Library, <https://www.nndc.bnl.gov/endl-b8.0/>.